Elements for Modeling Diffused Piezoresistor Temperature Coefficient and Sensitivity

Dragan Mladenovic, Jason Hutchins, Eddie Tran and Shifeng Lu

Motorola, 5005E. McDowell Rd., M/D D145
Phoenix, AZ 85008

ABSTRACT

This article reviews elements needed to be considered in order to improve accuracy of the temperature coefficient and sensitivity (span) simulation for diffused piezoresistors. Modeling is done through an algorithm developed in 'Mathematica'. Input parameters for the model are device doping profiles. The algorithm divides doping profile into finite elements that are considered infinitesimal, uniformly doped areas. The model was evaluated on a number of different experimental parts. The same test samples were used for electrical data gathering and SIMS analysis. The test devices had junction depths varied between 0.6 and 4 microns, and surface boron concentration between 5E17 cm-3 and 1E18 cm-3. Simulation results correlate very well with measurements.

Keywords: Diffused piezoresistors, temperature coefficients, span.

INTRODUCTION

Piezoresistivity is one of the widely exploited physical phenomenon in a variety of sensor devices. A first publication related to this material property, with the basic operating principle applicable to the wire and foil gages, dates back to 1856. That was the time when Lord Kelvin reported that certain metallic conductors subjected to mechanical strain exhibited a corresponding change in electrical resistance [1]. The physics of this phenomenon in semiconductors is somewhat different from that in metals, although the over-all effect is comparable. In general, semiconductors show a much larger percentage change in electrical resistance per unit of strain than metals do.

The intent of this article is to analyze simulation elements of piezoresistive devices for better correlation between semiconductor process parameters with the final transducer performance over temperature and pressure.

Basic Piezoresistive Principles

The piezoresistive effect is a name given to the change in electrical resistivity that occurs with application of mechanical stress. Thus piezoresistive transducers act as converters of external stress changes to proportional, measurable electrical signals.

In this work we are dealing with single crystal silicon (SCS) transducers thus the analysis of their properties will be based on solid state physics models. Conductivity in semiconductors depends on [2] (i) the degree to which the states are populated, (ii) their group velocity, (iii) their relaxation time, or more generally, the transition probabilities for scattering from these states to others. When the crystal is strained, any or all of these factors may change, and the resulting change in the sum of all the local contributions to the conductivity constitutes the piezoresistance effect.

In more generic terms, the scalar conductivity, σ, of p-type Si is related to the carrier concentration p and mobility μ by the following relation [3,4]:

$$\sigma = p \cdot \mu \cdot e, \qquad (1)$$

where e is the electronic charge. Hence, when stress is applied to an Si crystal, its conductivity can vary from either a change in the carrier concentration (p) or the mobility (μ). It is important to comment Eq. 2:

$$\left(\frac{1}{m^*}\right)_{ij} = \left(\frac{2\pi}{h^2}\right)\left(\frac{\partial^2 E(k)}{\partial k_i \cdot \partial k_j}\right), \qquad (2)$$

where h is Planck's constant and k_i are the Cartesian components of the wave vector **k**. This equation shows that the energy bands that have a high curvature, or second derivative of E(**k**), have a small effective mass. In a simple relaxation model the conductivity can be also expressed as:

$$\sigma = \frac{p \cdot e^2 \cdot \tau}{m^*} . \quad (3)$$

By combining (1) and (3) mobility can be expressed as:

$$\mu = \frac{e \cdot \tau}{m^*} . \quad (4)$$

From this prospective, piezoresistivity is a result of shifting or movement in k-space of the sub-bands when the crystal lattice strain changes. The final result is the hole mass change between light and heavy mass values. According to Eq. 4, mobility gets changed inversely. Externally these changes can be recorded by measuring device resistance change.

Piezoresistors are commonly defined by their piezoresistive coefficient, π. It specifies sensitivity of a particular device as a factor between applied stress and a relative change of the device resistance. Reported measurements [5,6] show a decrease of the piezoresistive effect with increasing temperature and increasing doping concentration In practice, sensitivity is often compromised to obtain a lower temperature coefficient.

EXPERIMENT

Manufacturing Components

Samples for the experiment were based on designs used for Motorola uncompensated pressure sensor products. Applied technology is standard bulk micromachining process for creating cavities from the back side of silicon [100] wafers (Fig. 1). Dimensions of the cavity size and diaphragm thickness are important mechanical components in defining the final device sensitivity over given pressure range.

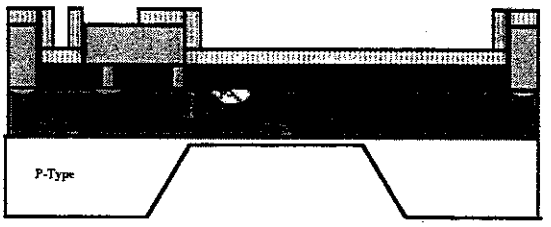

Fig. 1. Cross-section of the pressure sensor diffused piezoresistive transducer with cavity (not to scale).

Sensing transducers are compact structures in form of a Whetstone bridge positioned by one of the diaphragm edges (Fig.2).

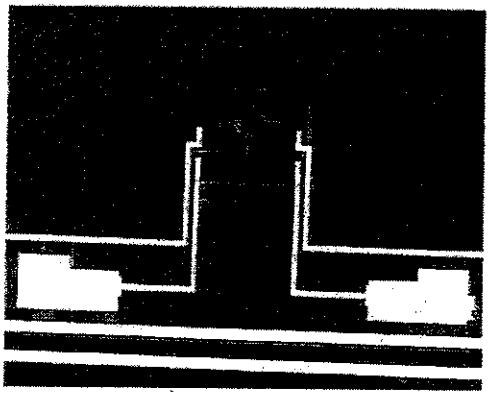

Fig.2 A typical compact transducer positioned by one of the diaphragm edges.

Process parameters varied in manufacturing test samples were: ion implantation dose, diffusion temperature and diffusion time. Table 1 lists details of these parameters for each of the sample groups. Samples numbered #1, 4 and 7 are 100 kPa parts. The next two groups (parts # 8 and 20) have larger cavities and designed for 10 kPa pressure range. The bottom group consists of four shallow junction (SJ) parts. The devices have the same cavity sizes as #8 and #20 groups, thus they are all low pressure (10 kPa) sensors too.

TABLE 1. List of samples with manufacturing details

	Implant dose	Diffusion
Sample group	[cm-2]	temp/time
1	1.28E+14	1180 C / 60'
4	1.28E+14	1160 C / 60'
7	1.38E+14	1160 C / 60'
8	1.12E+14	1160 C / 60'
20	1.12E+14	1200 C / 90'
SJ-4	3.00E+13	975 C / 30'
SJ-13	2.00E+13	975 C / 30'
SJ-15	3.00E+13	1050 C / 90'
SJ-3	2.00E+13	1050 C / 90'

After test sample wafers were processed, between 24 and 48 devices from each of the groups were assembled in order to measure thermal and electrical characteristics. The results

were statistically analyzed and average values per group are listed in Table 2.

Doping Profiles

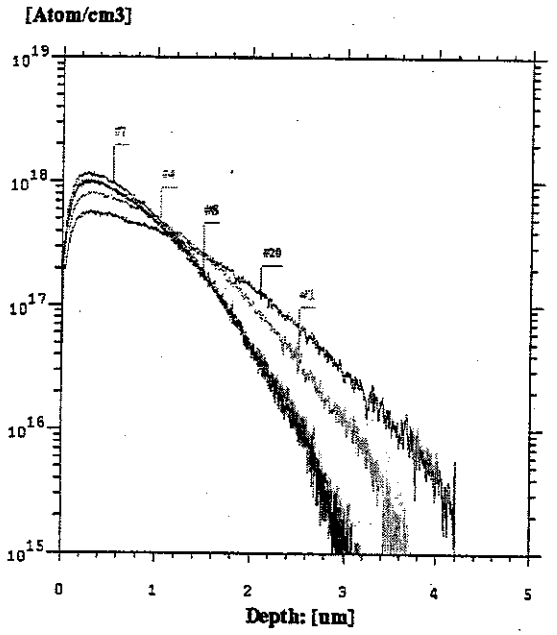

Fig . 3 SIMS profiles on diffused piezoresistors with junction depth >3 μm.

Table 2 Measured temperature coefficient and output span results.

Sample group	Tcr [%/C]	Span [mV]
1	0.3398	92.34
4	0.3126	93.68
7	0.3035	106.64
8	0.3546	39.99
20	0.3447	46.8
SJ-4	0.2417	42.83
SJ-13	0.291	58.98
SJ-15	0.3363	50.19
SJ-3	0.3898	50.97

Doping profiles for samples from all groups listed in Table 1 were received by using the state-of-the-art magnetic Secondary Ion Mass Spectrometry (SIMS) instrument, Cameca IMS-6f. A 15 KeV net impact energy Cs^+ primary ion beam was chosen for the boron depth profiling instead of conventional oxygen ion beam because the oxygen beam is known to induce roughening effect when the sputtering depth is greater than 1-2 μm. In addition, a molecular ion, $^{11}B^{28}Si^-$, is monitored with a high mass resolution (ΔM/M) of 2000 in the SIMS depth profiling in order to achieve a good dynamic range of boron profiles. At least two profiles for each wafer are obtained to verify the measurement results.

Fig. 3 and Fig. 4 illustrate SIMS profiles obtained from two groups, i.e. deep junctions (Xj ≥ 3 μm) and shallow junctions (≤ 1 μm), respectively. All profiles were obtained under the same experimental conditions to maintain high consistency in the measurements.

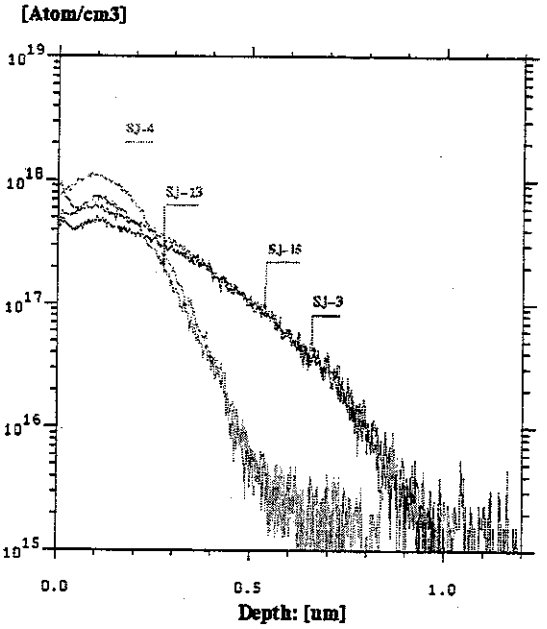

Fig. 4. SIMS profiles on diffused piezoresistors with junction depth <1 μm.

Electrical Characterization

Temperature coefficients were calculated from the measurements of the device resistance, R, over temperature. The temperatures used for this purpose were 125 C, -40 C and room temperature (25 C). The coefficients were calculated as follows:

$$Tcr = \frac{R[125C] - R[-40\,C]}{R[25\,C]\cdot 165}\cdot 100. \qquad (5)$$

The next parameter of interest is the output signal span over pressure. It was measured as the differential output voltage of the transducer when pressure changes from 0 kPa to 10 kPa or 100 kpa, respective to the sample group under test.

SIMULATION ALGORITHM

The simulation algorithm used here was based on the mobility of free carriers (holes in our p-type transducer). An effective value can be expressed as:

$$<\mu>=\frac{\int \mu(z)\cdot p(z)\cdot dz}{\int p(z)\cdot dz} \quad . \qquad (6)$$

Mobility is depicted with $\mu(z)$ for a position z from the surface. $p(z)$ represents hole concentration for the same location. Doping profiles (Fig. 3 and Fig. 4) were used as the input parameters for the algorithm to calculate effective mobility for each of experimental samples according to this equation. The algorithm is shown in Fig. 5.

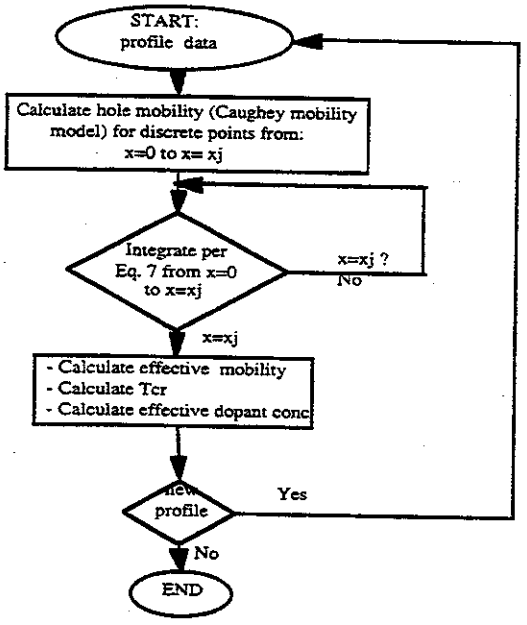

Fig. 5 Algorithm for calculating effective mobility, temperature coefficient and effective doping concentration.

The algorithm uses the Caughey model [8] for calculating mobility of the holes. This model was selected over the Arora model [9] because it has a better correlation with the tabulated mobility reported in [10]. After integrating along the doping concentration profile, an effective mobility for the entire profile is calculated per Eq. 5. The effective mobility result is then used back in the Caughey formula to solve it for an effective doping concentration. That would correspond to an adequate uniformly doped material that would have equivalent piezoresistive performance. The process is repeated for different ambient temperatures (room temperature, -40 C, and 125 C). Based on these results a temperature coefficient for the given profile is calculated (Eq. 6). Results of the calculations are listed in Table 3.

$$Tcr = \frac{<\mu>[125C] - <\mu>[-40\,C]}{<\mu>[25\,C]\cdot 165}\cdot 100. \quad (6)$$

Results of the procedure described above have only a relative correlation to the real sample parameters (Table 2 and 3). We propose the following explanation for this discrepancy. Originally used profiles in Eq. 5 to calculate effective mobility are the SIMS doping profiles. However, distribution profiles of the free carriers (holes) should be taken instead. Under influence

Table 3. Calculated effective mobility, temperature coefficients and effective doping concentration.

	Model 1		
	Eff mobil	Tcr	Effective dopant concentration
Sample group	[cm2/V-s]	[%/C]	[cm-3]
1	242	0.138	4.59E+17
4	228	0.114	5.56E+17
7	221	0.1	6.14E+17
8	229	0.1147	5.47E+17
20	269	0.185	3.20E+17
SJ-4	209	0.071	7.20E+17
SJ-13	238	0.122	4.86E+17
SJ-15	239	0.135	4.77E+17
SJ-3	268	0.181	3.25E+17

of the concentration gradient, holes have a diffusion component that pushes them deeper in the material and further from the surface. However, the final hole profile is defined by additional components and they are electrostatic forces from the boron ions as well as from the charges present in passivation layers (interface, fixed and mobile). When the two components (diffusion and drift) are balanced, then the final free carrier distribution is defined. Besides boron doping profiles, all other elements (passivation films and interface states) are parameters of the technology applied and process and material conditions.

$$\langle \mu \rangle = \frac{\int \mu_B(z) \cdot p_h(z) \cdot dz}{\int p_h(z) \cdot dz} \quad . \qquad (7)$$

Based on the discussion above, a correction factor for the hole distribution versus boron ion profile was applied. Since the two are different, a new equation was used for effective mobility (Eq. 7). Mobility of the carriers at a certain location is dependent on the scattering effects from doping ions and their concentration, thus we used the boron profile to get the mobility for each of the points z. The hole concentration is now different and has its one profile. That is depicted with index h in the equation. The model was ran again and received results are listed in Table 4. The last column shows ratio of the effective doping concentrations between the two models.

Table 4: Calculated effective mobility, temperature coefficients, effective dopant concentration and model1/model2 ratio for dopant concentration.

	Model 2 (carrier redistribution)			
	Eff mobil	Tcr	Effective dopant concentration	D.C. Model (2)/(1) ratio
Sample group	[cm2/V-s]	[%/C]	[cm-3]	
1	351	0.339	1.01E+17	0.22
4	338	0.31	1.22E+17	0.22
7	335	0.303	1.29E+17	0.21
8	356	0.351	9.30E+16	0.17
20	354	0.346	9.62E+16	0.30
SJ-4	309	0.246	1.87E+17	0.26
SJ-13	331	0.294	1.36E+17	0.28
SJ-15	348	0.333	1.05E+17	0.22
SJ-3	371	0.389	7.16E+16	0.22

DISCUSSION

Temperature Coefficient

In our discussion we will be using the ratio coefficient listed in the last column of Table 4. It is the ratio of the effective dopant concentration received form the two models. The lower the coefficient, the more distribution of holes happened relative to the boron profile.

(i) Let's start with samples that received just the activation energy after implantation (SJ-4 and SJ-13). Their profiles were mostly defined by the implantation process. This two devices have different implantation doses (by factor 1.5), but both were activated at the same temperature (975C for 30 min). Obviously (Fig. 3 and Table 4), the samples that received higher implantation dose (SJ-4) show more hole redistribution effect than the SJ-13 samples. The coefficient increases from 0.26 to 0.28, respectively.

(ii) The next pair of samples (SJ-15 and SJ-3) received also different implant doses but were diffused at higher temperature (1050 C) and for much longer time (90 min) than the previous pair of devices. Coefficients are now the same (0.22) for both SJ-15 and SJ-3 groups, but lower than for (i). It is also interesting to compare SJ-4 and SJ-15 groups. Both received the same implant dose but were diffused at different temperatures. The former one has a higher ratio coefficient, meaning less redistribution.

(iii) Let's review groups with deeper junctions now. They were processed through different diffusion processes flows. After that passivation layers were stripped off of their wafers and the final, new oxide layer is grown under the same conditions for all of the parts. Samples labeled #1, #4 and #7 have coefficients 0.22, 0.22 and 0.21, respectively. That means that final passivation and interface states and charges are very similar in these cases. And that is expected based on the same process flow.

(iv) Groups #8 and #20 show very different results from the rest of the test samples. Their coefficients vary from 0.17 to 0.30, although they have the same implantation dose and were supposed to receive the same final oxide treatment as devices in (iii). The suspicion is that something different happened to these parts than planned by the experiment. It can be caused by a different temperature treatment or

contamination level. It will be investigated further.

Output Signal Span

These results can be discussed only in generic terms since the signal output span performance has a limited dependence on the dopant concentration. Namely, more important is the mechanical aspect of the design that defines flexibility of the diaphragm over a pressure range. Mobility or dopant concentration can be just one of the elements for consideration here. However, if the mechanical components are the same and very repeatable among the parts, then concentration profiles get the dominant role in the final transducer response.

Relatively speaking, for the group with the deep junction parts it can be seen that their measured span tracks well with the effective mobility (Table 4). Namely, the higher mobility, the lower sensitivity, thus lower span output.

However, for the shallow junction parts results are random and there is no an obvious relation between electrical measurements and simulated results. We contribute this to the mechanical differences of the test samples that could not be controlled easily.

SUMMARY

Piezoresistive model proposed here is based on the free carrier mobility characteristics rather than on the piezoresistive constants of uniformly doped substrates. This major difference allowed us to simulate basic performance characteristics of diffused piezoresistive pressure sensors.

Nine different groups of test samples were manufactured. Temperature treatment of the samples was varied between the groups resulting in devices with shallow junctions from (0.6 μm) to relatively deep junctions (4 μm). All samples were tested and their temperature coefficients, spans and SIMS profiles were presented. The newly proposed model based on the weighted (effective) mobility over the entire doping profile was applied in order to simulate piezoresistive characteristics of the experimental parts. Simulation analyses were correlated to the measured values and results discussed.

It was showed that temperature coefficient and sensitivity of transducers can be modeled and their performance over temperature and pressure predicted. It is important to emphasize a limited applicability of the model on the device span characteristics since that can be predominantly defined by mechanical properties of the diaphragm and cavity. In absence of that variability, the model explained here can be used for relatively accurate prediction of the transducer characteristics.

Results presented in Table 4 suggest that performance of piezoresistive diffused devices can be evaluated through their free carrier profile characteristics. Therefore essential piezoresistive parameters, temperature coefficient and sensitivity, can be designed or simulated according to the semiconductor processes affecting dopant (and free carrier) concentration profiles. In order to have better model accuracy it is imperative to quantify all high temperature processes used in manufacturing these devices in terms of passivation and interface layer charges or their electric fields. This will help in calculating the exact hole distribution profile and thus predict more accurately their piezoresistive characteristics. Simulation results received from this model show a good correlation with experimental parts.

REFERENCES

1. J. Fraden, "AIP Handbook of Modern Sensors (Physics, Design and Applications)", American Institute of Physics, New York (1995).
2. C. Herring, "Transport Properties of a Many-Valley Semiconductor", Bell System Technical J., 34, 237, 1955.
3. S. Middelhoek, S.A. Audet, "Silicon Sensors", Academic Press, London (1989)
4. S.M. Sze, "Semiconductor Sensors", J.Willey&Sons, Inc., N.Y. (1994).
5. O.N. Tufte, et al., "Piezoresistive Properties of Silicon Diffused Layers", J. App. Phys., 34, 313 (1963).
6. C.S. Smith, "Piezoresistance Effects in Germanium and Silicon", Phys. Rev., 94, 42 (1956).
7. W.W. Hines and D.C. Montgomery, "Probability and Statistics in Engineering and Management Science", J. Wiley&Sons, N.Y. (1980).
8. D.M. Caughey et al., "Carrier Mobilities in Silicon Empirically Related to Doping", Proc. IEEE, vol.;. 55 (1967.
9. N.D. Arora, et al., "Electron and Hole Mobilities in Silicon as a Function of Concentration and Temperature", IEEE Trans. Electron Devices, vol. ED-29 (1982.
10. TMA TSUPREM-4, Version 6.2, Technology Modeling Associates Inc., 2-64 (1995).